

Controlling the Size of Microbubbles for Drag Reduction

T. Kawamura, *University of Tokyo*

A. Kakugawa, Y. Kodama, *National Maritime Research Institute*

Y. Moriguchi, H. Kato, *Toyo University*

Three different methods have been investigated for generating microbubbles to control the bubble diameter separately from the main flow velocity. The first two methods achieve this by adjusting the local shear stress where bubbles are generated, while the third method uses foaming of dissolved air to generate very small bubbles. The average diameter of bubbles was successfully controlled by the first two method within the range of 0.5–2 mm for the fixed main flow velocity of $U=3\text{m/s}$, while the very small bubbles of 20–40 μm were generated by the third method. The influence of the bubble diameter on the frictional drag reduction was investigated for a diameter range of 0.5–2 mm, and was found to be insignificant.

1. Introduction

Many experimental results have shown that microbubbles can reduce the frictional drag of a turbulent boundary layer by 20% - 80% [1-3]. Since generating microbubbles costs energy, it is necessary to optimize the size of bubbles and their distribution in the boundary layer to achieve a net gain. However, there is neither a theory nor sufficient experimental data for this goal.

Information on the effect of the size of microbubbles on the drag reduction is particularly limited, because it is not easy to control the size of bubbles in a boundary layer. The size of generated bubbles depends more on the wall shear stress than on the size of holes or the grain of the porous plate thorough which air is injected into a boundary layer [2]. This makes it difficult to control the mean flow velocity and the size of bubbles independently.

However, several experimental results suggest that small bubbles are more suitable for the drag reduction, although there is no conclusive evidence. The microbubble drag reduction was first reported by McCormick and Bhattacharyya[4]. They generated very small hydrogen bubbles by electrolyzing water, and reported 10 – 30% reduction of the frictional resistance. This reduction rate is very high considering the estimated void ratio of less than 1%. Gore and Crowe [5] have shown that solid particles either increase or decrease turbulent intensity of the carrier phase depending on the ratio of the particle size to the turbulence scale. This suggests that small bubbles may suppress

the liquid phase turbulence.

The objective of this study is to establish methods for controlling the size of microbubbles and to investigate the influence of the bubble size on the drag reduction. To investigate the effect of the bubble size, it must be controlled while maintaining the same mean flow velocity. For this purpose, we investigated three different methods. The first two methods are based on the fact that the bubble size depends on the mean wall shear stress[2]. In the first method a water-jet is used to control the local mean shear stress at the injection area, while in the second method the sectional area of the channel is locally changed where bubbles are generated. The bubble size obtained by these two methods ranges between 0.1mm – 2mm, while the third method targets the bubble size of 20 – 40 μm through foaming of dissolved water. The descriptions and experimental results for the three methods are presented in the following sections.

2. Tangential Water-jet

The diameter of bubbles generated by injecting air into a turbulent boundary layer through array of holes or porous medium depends on the mean shear stress at the wall. Therefore, one way to control the bubble diameter is to increase or decrease the local mean shear stress at the wall where air is injected. This is achieved by two different methods in this study. The first one described in this section uses a tangential water-jet to increase the local shear stress

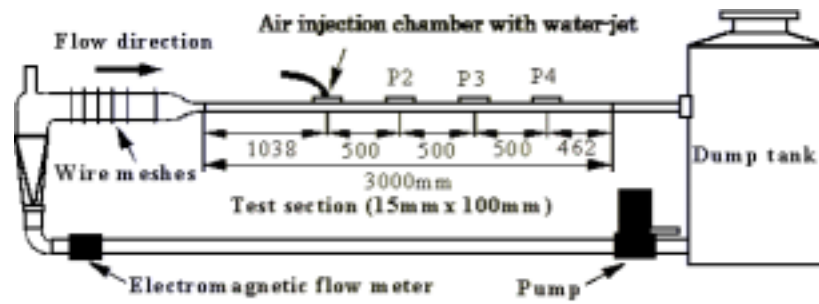


Fig. 1 Setup of the experiment at National Maritime Research Institute, in which the water-jet system is used for controlling the bubble size.

on the plate with array of holes through which air is injected. Fig. 1 shows the setup of the experiment carried out at National Maritime Research Institute, and Fig. 2 shows a close view of the tangential water-jet system. The inner diameter of the air injection holes is 0.5mm. The channel is made of transparent acryl resin so that optical measurements and observation of bubbles are possible. The test section is 15mm in height, 100mm in width, and 3000mm in length. The air injection chamber with the water-jet system is attached to the top wall. The results for the bulk mean velocity of $U=3\text{m/s}$, and the water-jet flow rate of $Q=0 - 30 \text{ l/min}$ are presented in this paper. The ratio of the water-jet flow rate to that of the main flow is 1:9 at $Q=30 \text{ l/min}$

Fig. 3 shows the profiles of the mean velocity at a section 500mm downstream from the air injection chamber ($X=500\text{mm}$). The asymmetric velocity profiles indicate that the influence of the jet does not disappear before $X=500\text{mm}$ ($X/H = 33.3$, with H being the channel height). The effect of the water-jet on the bubble diameter is very clearly observed in Fig. 4, in which pictures of bubbles at five different downstream positions are shown. The average bubble diameter at $X=100\text{mm}$ without the water-jet injection is about 2mm, while that with the water-jet is smaller than 0.5 mm. The bubble diameter grows in the downstream direction, but the difference in the diameter persists at $X=1500\text{mm}$ ($X/H=100$). As the bubbles are carried downstream, the water-jet is diffused and the local shear stress decreases. Probably, the bubble diameter approaches an “equilibrium diameter” which is a function of the local shear stress.

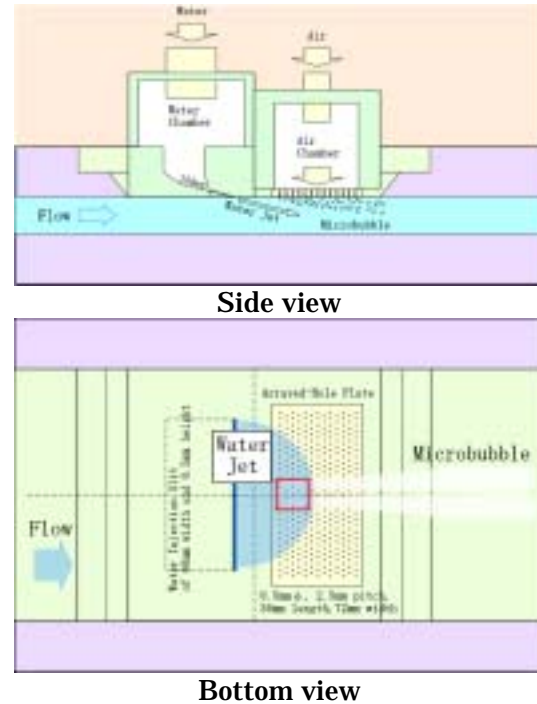


Fig. 2 The tangential water-jet system used for controlling the bubble size.

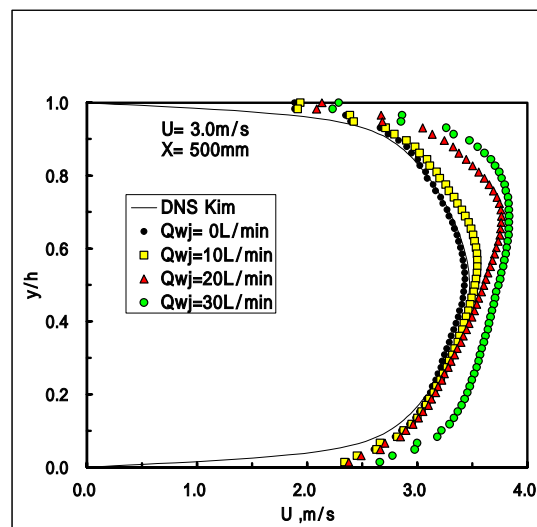


Fig.3 Profiles of mean velocity at $X=500\text{mm}$ with tangential water-jet injection

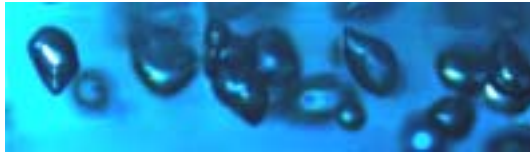
U=3m/sec Water jet=0 l/min



X=100mm



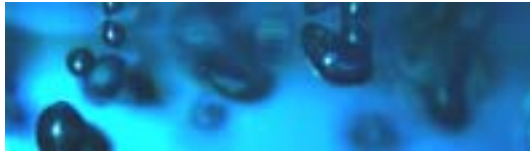
X=300mm



X=500mm



X=1000mm



X=1500mm



0 5 10 15 20mm

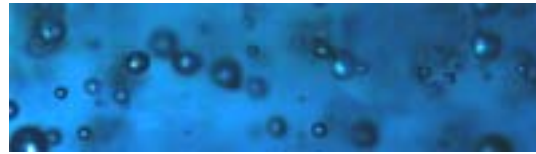
Water jet=30 l/min



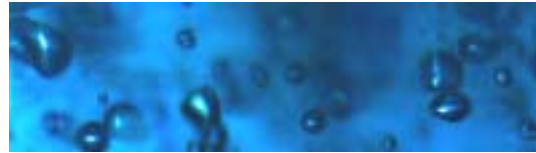
X=100mm



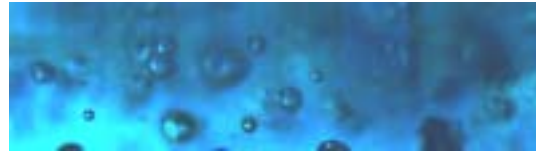
X=300mm



X=500mm



X=1000mm



X=1500mm

Fig. 4 Pictures of bubbles showing the effect of the tangential water-jet on the bubble diameter and its persistence in the downstream direction. The mean velocity U is 3 m/s, and the mean void ratio α is 1%. X denotes the distance from the air injection chamber.

3. Changing the Size of Test Section

In the second approach, three different channels were used to control the bubble diameter. Fig. 5 shows the three channels, and Fig. 6 shows the setup of the experiment carried out at Toyo University. The three channels have the test sections of the same size, 10mm in height, 100mm in width, and 2000mm in length, but the height at the air injection port is different. By use of the three different channels, the local shear stress at the air injection port can be controlled without changing the mean velocity in the test section. Air is injected through a porous plate mounted on the upper surface of the air injection section.

Fig. 7 shows photographs of bubbles taken from the top of the test section of Channel 2 and 3 at $X=750\text{mm}$, with X denoting the distance from the air injection port. The mean velocity in the test section was 5m/s and the mean void ratio α was 10%. Channel 3 has four times larger sectional area at the air injection port than Channel 2, so the local mean shear stress is estimated to be an order of magnitude larger for the same mean velocity in the test section. The pictures clearly exhibit the effect on the bubble diameter. By processing many pictures by software, the bubble size distributions shown in Fig. 8 were obtained. As the mean flow velocity is decreased, the

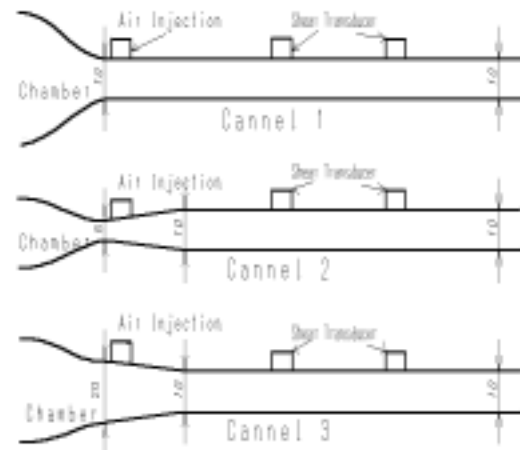


Fig. 5 Three channels with different height at the air injector. Dimensions are in millimeters

average diameter increases, and the distribution becomes more scattered. This result is consistent with the previous studies [2, 3]. Fig. 9 shows the relation between the mean flow velocity and the average bubble diameter for the same condition of $\alpha=10\%$ in three different channels. In all channels, the average diameter decreases as the mean flow velocity is increased, but the difference among the channels is larger at lower velocity. The change in the average diameter is largest in Channel 3 suggesting that the large bubbles are split into small ones in the

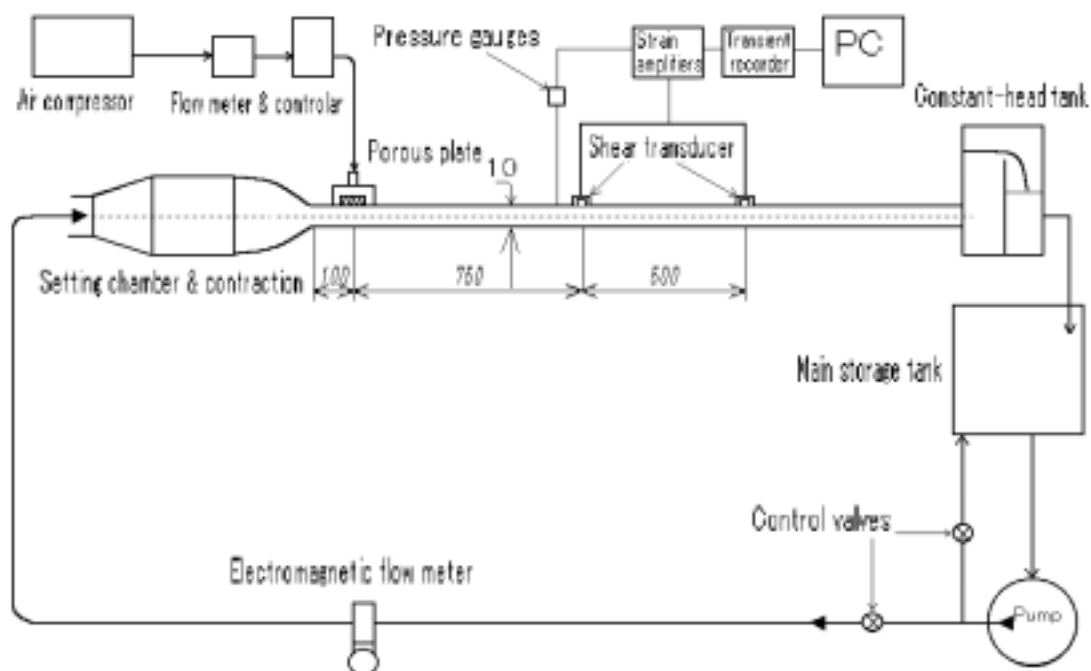
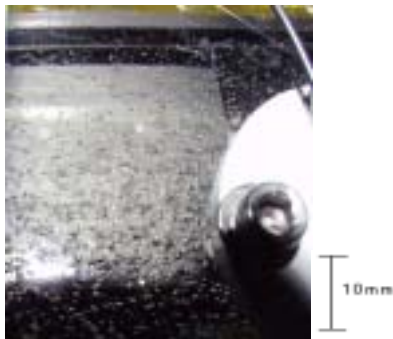


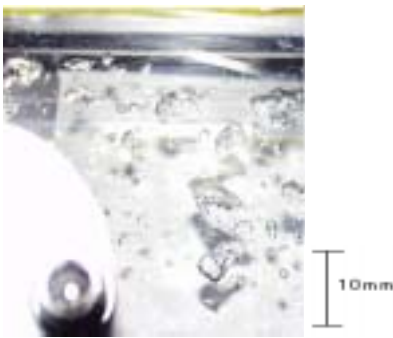
Fig. 6 Setup of the experiment at Toyo University using different channels for controlling the bubble size. Dimensions are in millimeters.

test section since the mean shear rate in the test section is larger than at the air injector. On the other hand, the average bubble size in Channel 1 and 2 is much less dependent on the mean velocity, and the difference between the two channels seems to persist even if the velocity is increased. These facts indicate that the size of a bubble depends on the highest shear stress that the bubble has experienced.

The effect of the bubble size on the drag reduction rate was examined in Fig. 10 using the wall shear stress measured by shear transducers mounted flush on the upper surface of the test section at the streamwise locations shown in Fig. 6. The nondimensionalized frictional drag C_f/C_{f0} for various flow velocities and for different channels are plotted versus the mean void ratio. Although the data are for various bubble diameters ranging from 0.5 mm to 2mm, the points are concentrated near the mean line. This indicates that the influence of the bubble diameter is small within this diameter range. It is probably concluded that the influence of the bubble diameter is small when the diameter is sufficiently large compared with the characteristic scale of turbulence.



(a) Channel 2



(b) Channel 3

Fig. 7 Pictures of microbubbles in different channels. (a) Channel 2, (b) Channel 3.

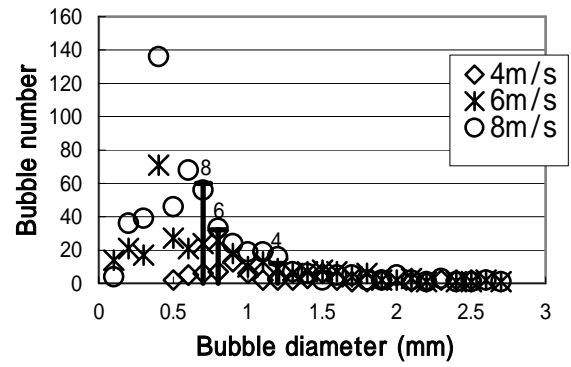


Fig. 8 Histogram of the bubble diameter at $X=750\text{mm}$ of Channel 1. The mean void ratio is 10%. The bold lines indicate the mean diameter for each mean velocity.

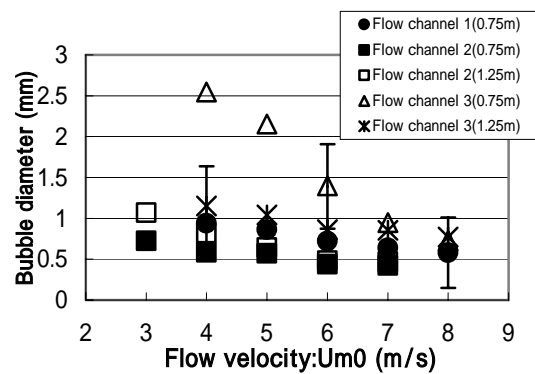


Fig. 9 Average bubble versus mean velocity. The void ratio is 10%.

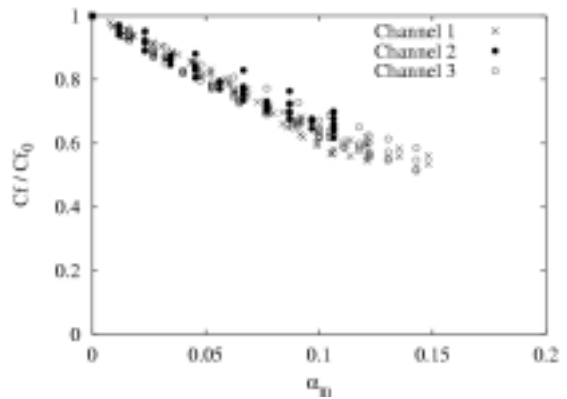


Fig. 10 Reduction of frictional drag by microbubbles in different channels and at different flow velocities.

4. Foaming of dissolved air

The previous investigations have shown that the influence of the bubble size on the drag reduction is negligibly small within the investigated range of bubble diameter. However, there is still a prospect that bubbles that are sufficiently small compared to the characteristic scale of turbulence may significantly influence the drag reduction rate. Therefore, we investigated a method to generate bubbles of $20\ \mu\text{m} - 40\ \mu\text{m}$ in diameter. Bubbles of this size are utilized for mixing and separation processes, and are usually generated by foaming microbubbles from air dissolved in liquid [6]. Since the microbubble drag reduction requires higher void ratio than other applications such as mixing or separation, we investigated whether this method is applicable to the purpose of drag reduction.

Fig. 11 shows the test section used in the experiment carried out at University of Tokyo. The test section is $120 \times 50 \times 580$ in height, width, and length respectively. Sufficiently aerated water under the absolute pressure of $P_1 = 0.8\text{MPa}$ in a pressure tank is introduced into the test

section through a slit. The water from the pressure tank is depressurized to the absolute pressure level inside the test section $P_0 = 0.1\text{MPa}$ at the valve installed before the slit. Since the solubility of air in water is proportional to the pressure, the excess air is separated and makes microbubbles. The estimated void ratio α obtained by this procedure is given by

$$\alpha = \frac{C(P_1 - P_0)}{P_0 + C(P_1 - P_0)},$$

in which C is solubility of air in water (cm^3/cm^3), which is 0.02 under $P_0 = 0.1\text{MPa}$ at the temperature of 20°C . The void ratio α is estimated to be about 0.12 for $P_1 = 0.8\text{MPa}$.

In order to measure the diameter of bubbles, the depressurized foaming water was introduced to a thin channel to which a microscope was mounted. Fig. 12 shows an example of picture through the microscope. The bubble diameter measured on the pictures by hand is shown in a histogram in Fig. 13. The shape of the distribution is similar to that shown in Fig. 8 for bubbles generated by shear stress, but the range of

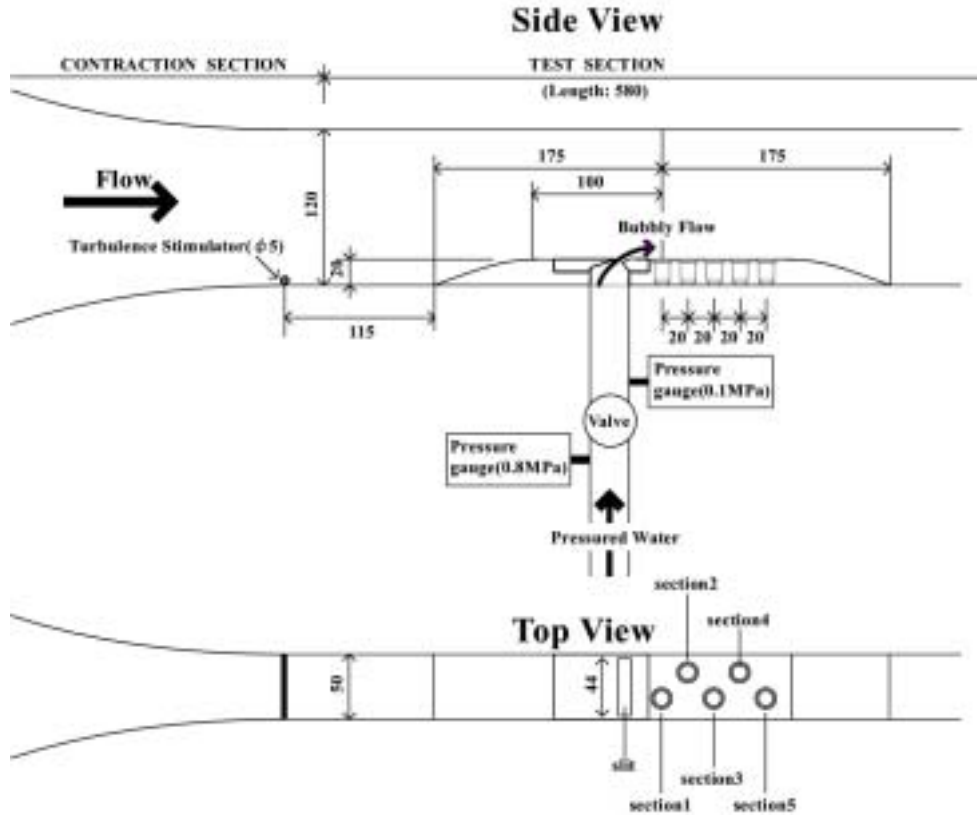


Fig. 11 Test section used in the experiment at University of Tokyo. Bubbles are generated by decompressing aerated water. Dimensions are in millimeters.

the diameter is an order of magnitude smaller. The most frequent diameter range is between 20 and 40 μm , which includes one out of two bubbles, and the calculated average diameter was 47 μm . The void ratio estimated from the bubble number distribution and the depth of the picture was about 5% which is on the same order as the value estimated from the solubility of air in water.

This foaming water is introduced into the turbulent boundary layer inside the test section through a slit at the rate of $Q=5 - 15$ l/min. Fig. 14 (a) shows a picture of bubbles in the test section near the injection point at the free-stream velocity of $U=1.5$ m/s, and the flow rate $Q = 10$ l/min. A picture of bubbles generated by injecting air through a porous plate at the same free-stream velocity is shown in Fig. 14(b) for comparison. The bubbles generated by the present method look more like cloud or smoke. Due to the limitation of the apparatus, it was impossible to measure the bubble diameter distribution accurately in

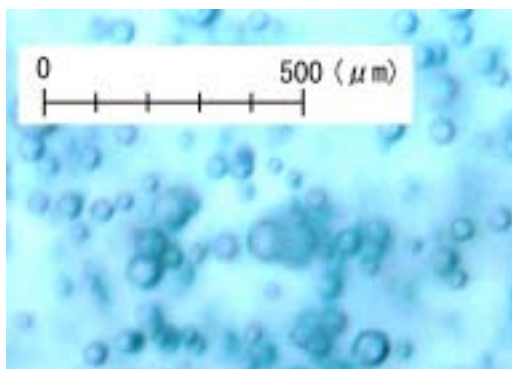


Fig. 12 Picture of bubbles generated by foaming of dissolved air in water.

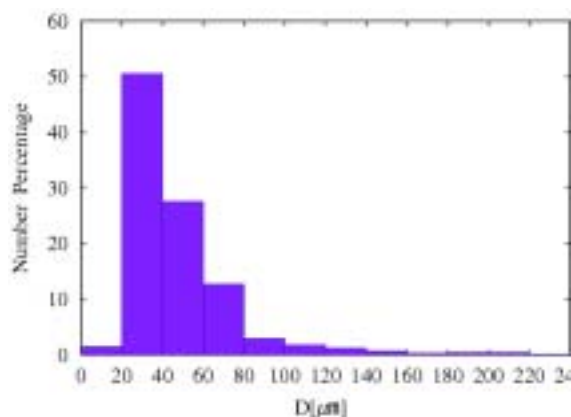


Fig. 13 Histogram of the size of bubbles generated by foaming of dissolved air in water.

the test section. However the appearance of bubbles was very similar to that in the channel for microphotography suggesting that the bubble diameter distribution is also similar. It was also noted that the appearance of the bubble cloud was not dependent on the free-stream velocity.

The profiles of the local void fraction at $X=40\text{mm}$ for a flow rate of $Q = 15$ l/min are shown in Fig. 15. The local void fraction was measured by the same optical sensor used by Guin et al.[2]. The peak void fraction is 2 – 3%, which is sufficiently high to cause a drag reduction. The shape of the profiles for $U = 4\text{m/s}$ and $U = 6\text{m/s}$ are very similar to



(a) Injection of foaming water



(b) Air injection through a porous plate

Fig. 14 Pictures of bubbles at the injection point in the test section. Main flow velocity is 1.5 m/s, and the flow rate of foaming water is 10 l/min.

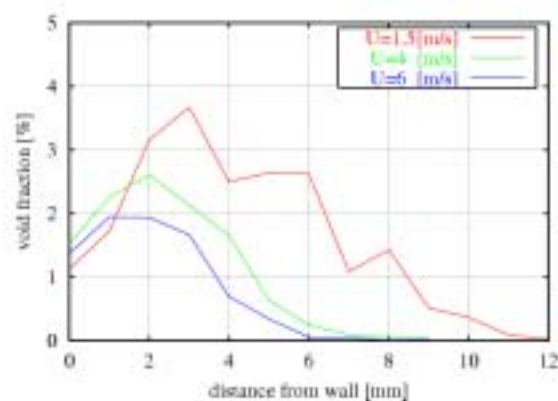


Fig. 15 Profile of the local void ratio at $X=40\text{mm}$. The flow rate of foaming water is 15 l/min.

those obtained by Guin et al. using a conventional way of bubble generation, but the profile for $U = 1.5$ m/s is a little different. The peak is shifted away from the wall, and the distribution is wider due to the influence of the injection velocity. The injection velocity is given by Q divided by the slit area, and is about 1.8 m/s at $Q = 15$ l/min. The result in Fig. 15 indicates that the influence of the injection on the velocity profile in the boundary layer is significant when injection velocity is comparable with the free-stream velocity.

The effects of the small bubble diameter are planned to be investigated using a long channel realizing a fully developed boundary layer. The bubble diameter of 20 – 40 μm corresponds to 5 – 10 viscous units in a fully developed boundary layer in a channel of $H=15\text{mm}$ and $U=6\text{m/s}$. Typical bubble diameter obtained by the air injection at the same condition is about 1mm, or 245 in viscous units. The ratio of the bubble diameter to the characteristic scale of turbulence may be small enough with the small bubbles generated by the present method.

5. Conclusions

In this study, we investigated three different methods to control the bubble diameter independently from the main flow velocity. The first two methods achieve this by adjusting the local shear stress where bubbles are generated, while the third method uses foaming of dissolved air to generate very small bubbles.

It has been shown that the average bubble diameter for fixed main flow velocities can be controlled within the range of 0.5 – 2 mm by the first two methods, and that the average diameter of 0.047 mm can be obtained by the third method. As bubbles flow downstream, the average diameter converges to an equilibrium value decided by the local shear rate due to coalescence and splitting. The present results indicates that splitting takes place in a short distance (on the order of $\delta - 10\delta$, with δ being the boundary layer thickness), while coalescence takes place in a much longer distance (on the order of 100δ). This means that the controlled diameter can be sustained over a distance of $L \sim 100\delta$, if the target diameter is smaller than the equilibrium value.

The effect of the bubble diameter on the drag reduction rate was found to be

insignificant for the diameter range of 0.5 – 2mm. This suggests that the bubble diameter is not an important parameter at least when the diameter is large compared with the characteristic scale of turbulence. However, the effect at the lower diameter range has not been clarified yet. The present study shows that the third method can be used for the investigation.

By use of the present methods, the bubble size is no longer dependent on the free-stream velocity, therefore it is now possible to investigate low Reynolds number bubbly flow for which a direct numerical simulations is possible. Comparisons between experiments and direct numerical simulations will be a very powerful way of investigating the interaction between microbubbles and turbulent boundary layer.

Acknowledgement

This study was partially supported by SR239 Research Committee of the Shipbuilding Research Association of Japan. Their financial support is greatly appreciated.

References

- [1] Madavan NK, Deutsch S, Merkle CL (1984) Reduction of turbulent skin friction by microbubbles. *Phys Fluids* 27:356-363
- [2] Guin M M, Kato H, Yamaguchi H et al (1996) Reduction of skin friction by microbubbles and its relation with near-wall bubble concentration in a channel. *J Mar Sci Technol* 1:241-254
- [3] Kato H, Miura K, Yamaguchi H et al (1998) Experimental study on the microbubble ejection method for frictional drag reduction. *J Mar Sci Technol* 3:122-129
- [4] McCormick ME, Bhattacharyya R (1973) Drag reduction of a submersible hull by electrolysis. *Nav Eng J* 85:11-16
- [5] Gore, R. A., and Crowe, C. T. (1989) Effect of particle size on modulating turbulent intensity, *Intern J Multiphase Flow*, Vol. 15, No. 2, pp. 279--285.
- [6] Kashiwa, M., Nakayama, M., Machiya, K., and Morita, K. (1997) Generating of the fine bubble by using pressurized line mixing, *J Japan Soc Mech Eng* No.974-1, pp 4-9, 4-10